Egypt. J. Chem. **Vol. 65,** No. 9 pp. 715 - 722 (2022)

Egyptian Journal of Chemistry

http://ejchem.journals.ekb.eg/

Entropy generation and nanoparticles cu o effects on mhd peristaltic transport of micropolar non-newtonian fluid with velocity and temperature slip conditions

Aya M. Ismael [a*], Nabil T. Eldabe [b], Mohamed Y. Abou zeid [b], and Sami M. El Shabouri [a]

[a] *Department of Mathematics, Faculty of Science, Ain shams University, Abbasiya, Egypt*

[b] *Department of Mathematics, Faculty of Education, Ain Shams University, Roxy, Cairo, Egypt*

Abstract

The present paper analyzes the influences of entropy generation as well as slip velocity and temperature conditions on MHD micropolar biviscosity nanofluid flow through a porous medium in a channel with peristalsis. The fluid effects of mixed convection, radiation, viscous dissipation and thermal micropolar properties are taken into consideration. The assumptions of low-Reynolds number and long-wavelength are used to simplify the governing equations of this problem. A semi-analytical solutions of these equations are obtained by using homotopy perturbation method. Moreover, the entropy generation is obtained in this study. Results are discussed for various parameters of the problem and depicted graphically. Physically, our model is consistent with the motion of digestive juice in the bowel whenever we are going to insert an endoscopy through it.

Keywords: Entropy generation; nanofluid; Peristaltic flow; mixed convection; porous medium.

1. Introduction

Micropolar fluids is called polar fluids with nonsymmetric stress tensor with microstructure. This model is established from the Navier-Stokes model. Ouaf and Abou-zeid [1] discussed micropolar properties and the electromagnetic on biviscosity fluid flow with mass and heat transfer through a porous non-Darcy medium. The effect of micromagnetorotation (MMR) of a Hartmann micropolar flow on the heat transfer has been studied by Aslani and Sarris [2]. Eldabe et al. [3] studied the motion of non-Newtonian fluid with mass and heat transfer a shrinking plate through porous medium. The importance of suction/injection for gravity modulation mixed convection is investigated due to an inclined sheet in micropolar fluid flow in the presence of thermal radiation and magnetic field by Ali et al. [4]. Abou-zeid [5] studied the peristaltic motion of non-Newtonian incompressible micropolar nanofluid in a two-dimensional asymmetric channel with heat transfer with taking consideration long-wavelength. The effect of microrotation viscosity on turbulent flows by taking a substitute formulation of the Navier–Stokes equation is discussed by Sofiadis and Sarris [6]. Recently, there are many researchers related to micropolar fluid over different surfaces [7- 10].

A nanofluid is containing nanometer-sized particles called nanoparticles, which are colloidal suspensions and typically made of oxides, metals, carbon nanotubes or carbides, include oil, water and ethylene glycol. Eldabe et al. [11] studied the effects of diffusion thermo and thermal diffusion on non-Newtonian nanofluid flow which containing microorganisms gyrotactic in the boundary layer. A study comprehensive on whether nanofluids present a net environmental benefit and is presented perspective environmental of this body of literature, this study also focused areas for future work by Mahian et al. [12]. Ouaf and Abou-zeid [13] discussed the problem of unsteady squeezing flow of a non-Newtonian nanofluid through a porous medium between two parallel plates,. The peristaltic motion of steady non-Newtonian nanofluid flow through a non-uniform inclined channel with heat transfer has been discussed by Eldabe et al. [14]. Vallejo et al. [15] discussed experimentally the corresponding mono nanofluids and hybrid nanofluids for two-phase and single-phase for convective heat transfer applications. The effect of

* Corresponding author should be addressed: ayaismael1990@gmail.com .; (A.M. Ismael).

Receive Date: 04 February 2022, Revise Date: 22 March 2022, Accept Date: 23 March 2022

DOI: 10.21608/EJCHEM.2022.120066.5388

Cattaneo-Christov heat flux of biviscosity nanofluid between two rotating disks on MHD flow through a porous media is studied by Abou-zeid [16]. Many results of the nanofluid are studied in these articles [17-21].

Entropy generation is the quantity of entropy which is constructed in any irreversible procedure such as mass and heat transfer processes including motion of heat exchange, bodies, substances mixing or expanding, fluid flow, anelastic deformation of solids, and any irreversible thermodynamic cycle, inclusive of thermal machines such as heat engines, power plants, heat pumps, air conditioners and refrigerators. Salimath and Ertesvag [22] discussed premixed H_2-air flames in a one-dimensional wall-bounded composition. Across a rocket engine a 2D flow of nanofluid with entropy generation and Bejan number is studied by Farooq et al. [23]. Chen and Jian [24] examined from conjugate two-layer thermal flow technique the entropy generation depending on minimization of entropy generation. Thermal radiation and the influences of entropy generation in a tapered channel on peristaltic blood flow of a micropolar-Magneto fluid were been discussed by Asha and Deepa [25]. Darbari et al. [26] studied entropy generation and the thermal–hydraulic numerically inside a plate-fin triangular duct for a nanofluid flow. Joule heating and impacts of an inclined magnetic field in a complaint walls channel are discussed on peristalsis by Hayat et al. [27]. Recently, there are different studies that discussed the entropy generation [28-29].

In this problem, we have analyzed the effects of entropy generation and both velocity and temperature slip conditions on MHD micropolar biviscosity nanofluid flow in a peristaltic channel through a porous medium. The fluid flows are in the presence of mixed convection, radiation, viscous dissipation, and thermal micropolar properties effects. The governing equations of flow are simplified under assumptions of low-Reynolds number and long-wavelength. Homotopy perturbation technique is used to obtain a semi-analytical solutions for the momentum, angular momentum, energy and nanoparticles concentration equations. Furthermore, the entropy generation is obtained in order to control problem physical parameters. Results are discussed for some parameters of the problem and sketched graphically. Physically, our model matches the motion of the digestive juice in the intestine when we insert an endoscope through it.

2. Mathematical description

The model of this problem is studied in Cartesian coordinates (x, y). Also, the wall of channel can be expressed as

$$h(X,t) = d_1 + a_1 \cos\frac{2\pi}{\lambda}(X - ct), \tag{1}$$

The equations governing the motion of this model can be represented as

$$\frac{\partial U}{\partial X} + \frac{\partial V}{\partial Y} = 0, \tag{2}$$

$$\rho_f\left(\frac{\partial}{\partial t} + U\frac{\partial}{\partial X} + V\frac{\partial}{\partial Y}\right)U = -\frac{\partial P}{\partial X} + \frac{(2\mu_f(1+\alpha^{-1})+k_1)}{2}\left(\frac{\partial^2}{\partial X^2} + \frac{\partial^2}{\partial Y^2}\right)U + \rho_f g\beta_T(T - T_0) - \rho_f g\,\beta_f(F - F_0) - \left(\sigma B_0^2 + \frac{\rho\nu}{k}\right)U + k_1\frac{\partial N}{\partial y}, \tag{3}$$

$$\rho_f\left(\frac{\partial}{\partial t} + U\frac{\partial}{\partial X} + V\frac{\partial}{\partial Y}\right)V = -\frac{\partial P}{\partial Y} + \frac{(2\mu_f(1+\alpha^{-1})+k_1)}{2}\left(\frac{\partial^2}{\partial X^2} + \frac{\partial^2}{\partial Y^2}\right)V - k_1\frac{\partial N}{\partial X}, \tag{4}$$

$$\begin{aligned}(\rho c)_f\left(\frac{\partial T}{\partial t} + U\frac{\partial T}{\partial X} + V\frac{\partial T}{\partial Y}\right) &= k_f\left(\frac{\partial^2 T}{\partial X^2} + \frac{\partial^2 T}{\partial Y^2}\right) \\ &+ \frac{(2\mu_f(1+\alpha^{-1})+k_1)}{2}\left[2\left(\frac{\partial U}{\partial X}\right)^2 + 2\left(\frac{\partial V}{\partial Y}\right)^2 + \left(\frac{\partial U}{\partial Y} + \frac{\partial V}{\partial X}\right)^2\right] \\ &+ \tau\rho_f c_f\left[D_B\left(\frac{\partial T}{\partial X}\frac{\partial F}{\partial X} + \frac{\partial T}{\partial Y}\frac{\partial F}{\partial Y}\right) + \frac{D_T}{T_m}\left(\frac{\partial T}{\partial X} + \frac{\partial T}{\partial Y}\right)^2\right] \\ &+ 2k_1\left[N^2 - N\left(\frac{\partial V}{\partial X} - \frac{\partial U}{\partial Y}\right)\right] \\ &+ \bar{\gamma}\left[\left(\frac{\partial N}{\partial X}\right)^2 + \left(\frac{\partial N}{\partial Y}\right)^2\right] \\ &- \frac{\partial q}{\partial Y},\end{aligned} \tag{5}$$

$$\rho J\left(\frac{\partial N}{\partial t} + U\frac{\partial N}{\partial X} + V\frac{\partial N}{\partial Y}\right) = -2k_1 N + \bar{\gamma}\left(\frac{\partial^2 N}{\partial X^2} + \frac{\partial^2 N}{\partial Y^2}\right) + k_1\left(\frac{\partial V}{\partial X} - \frac{\partial U}{\partial Y}\right), \tag{6}$$

$$\left(\frac{\partial}{\partial t} + U\frac{\partial}{\partial X} + V\frac{\partial}{\partial Y}\right)F = D_B\left(\frac{\partial^2}{\partial X^2} + \frac{\partial^2}{\partial Y^2}\right)F + \frac{D_T}{T_m}\left(\frac{\partial^2 T}{\partial X^2} + \frac{\partial^2 T}{\partial Y^2}\right), \tag{7}$$

Consider a wave frame (x, y) which moves with speed$c$. In wave frame, the coordinates and velocity components are related by the following transformations

$$\bar{x} = X - c\bar{t}, \bar{y} = Y, \bar{u} = U - c, \bar{v} = V, \bar{p}(x,y) = P(X,Y), \tag{8}$$

The radiative heat flux is given by

$$q = \frac{-4\sigma^*}{3k_R}\frac{\partial T^4}{\partial y}$$

Where $\sigma^*$is the Stefan Boltzmann constant and k_R is the mean absorption coefficient. We consider the temperature variance within the flow are sufficiently small such that T^4 may considered as a linear function

of temperature. This is accomplished by expanding T^4 in a Taylor series about T_1 and neglecting the higher-order terms, one gets

$$T^4 \approx 4T_1^3 T - 3T_1^4$$

Dimensionless quantities can be written as

$$x = \frac{\bar{x}}{\lambda}, y = \frac{\bar{y}}{d_1}, u = \frac{\bar{u}}{c}, v = \frac{\bar{v}}{c\delta}, \delta = \frac{d_1}{\lambda}, \gamma = \frac{\bar{\gamma}}{d_1^2\ \mu_f}, h = \frac{\overline{h_1}}{d_1}, a = \frac{a_1}{d_1}, N = \frac{d_1 \bar{N}}{c}, J = \frac{\bar{J}}{d_1^2}$$

$$\theta = \frac{T-T_0}{T_0},\ \varphi = \frac{F-F_0}{F_0},\ \mathrm{p} = \frac{d_1^2\,\bar{P}}{c\ \mu_f \lambda},\ G_t = \frac{\rho_f \mathrm{g} \beta_t\, T_0\, d_1^2}{\mu_f\, c},$$

$$G_f = \frac{\rho_f\, \mathrm{g}\, \beta_f\, F_0\, d_1^2}{\mu_f c}, P_r = \frac{\mu_f c_f}{k_f},\quad E_c = \frac{c^2}{c_f T_0}, R_e = \frac{\rho c d_1}{\mu_f}, N_t = \tau \frac{T_0 D_T}{\nu T_m},\ N_b = \tau \frac{F_0 D_B}{\nu},\ R = \frac{4\sigma^* T_1^3}{k_f k_R}. \quad (9)$$

According to these transformations, neglecting the bar mark and after applying $\delta \ll 1$, the system of equations can be written as follows:

$$\frac{\partial p}{\partial x} = \left((1+\alpha^{-1}) + \frac{\beta}{2}\right)\frac{\partial^2 u}{\partial y^2} + \beta \frac{\partial N}{\partial y} - \left(M + \frac{1}{Da}\right)u + G_t\theta - G_f\varphi, \quad (10)$$

$$\frac{\partial p}{\partial y} = 0, \quad (11)$$

$$\left(1+\frac{4}{3}R\right)\frac{\partial^2 \theta}{\partial y^2} + \frac{E_c P_r}{R_e}\left((1+\alpha^{-1}) + \frac{\beta}{2}\right)\left(\frac{\partial u}{\partial y}\right)^2 + P_r\, N_t \left(\frac{\partial \theta}{\partial y}\right)^2 + P_r\, N_b \left(\frac{\partial \theta}{\partial y}\right)\left(\frac{\partial \varphi}{\partial y}\right) + \frac{2\,\beta\, E_c}{R_e}\left[N^2 + N\frac{\partial u}{\partial y}\right] + \gamma \frac{E_c P_r}{R_e}\left(\frac{\partial N}{\partial y}\right)^2 = 0, \quad (12)$$

$$2\beta N - \gamma \frac{\partial^2 N}{\partial y^2} + \beta \frac{\partial u}{\partial y} = 0, \quad (13)$$

$$\frac{\partial^2 \varphi}{\partial y^2} + \frac{N_t}{N_b}\frac{\partial^2 \theta}{\partial y^2} = 0, \quad (14)$$

The appropriate boundary conditions are

$$\frac{\partial u}{\partial y} = 0,\quad N = 0,\quad \theta = 0,\quad \varphi = 0 \quad \text{at} \quad y = 0,$$

$$u + \beta_1 \frac{\partial u}{\partial y} + \beta_2 \frac{\partial^2 u}{\partial y^2} = -1,\quad N = 1,\quad \theta + \gamma_1 \frac{\partial \theta}{\partial y} = -1,\quad \varphi = 1 \quad \text{at} \quad y = h \quad (15)$$

3. Entropy generation analysis

The main aim of the present study is to minify entropy generation to obtain better results by restricting physical parameters of the problem. The dimensionless form of entropy generation can be exhibited mathematically as follows [3]:

$$Eg = \left(1+\frac{4}{3}R\right)\left(\frac{\partial \theta}{\partial y}\right)^2 + \frac{E_c\, P_r}{R_e}\left((1+\alpha^{-1}) + \frac{\beta}{2}\right)\left(\frac{\partial u}{\partial y}\right)^2 + P_r N_t \left(\frac{\partial \theta}{\partial y}\right)^2 + P_r\, N_b \frac{\partial \theta}{\partial y}\frac{\partial \varphi}{\partial y} + \frac{E_c\, \beta}{R_e}\left(N^2 + N\frac{\partial \theta}{\partial y}\right) + \gamma \frac{E_c\, P_r}{R_e}\left(\frac{\partial N}{\partial y}\right)^2, \quad (16)$$

4. Method of Solution

The governing equations are solved by using the homotopy perturbation method which is useful method to solve many ordinary or partial differential equations. It follows only a few steps to obtain semi-analytical (series) solutions for non-linear differential equations. Furthermore, the obstacles of the well-known perturbation method are removed by a collection of the perturbation method and the homotopy analysis technique, while keeping all their features. First, we devise a suitable homotopy equation. Following [33], Eqs. (10)-(14) can be formulated as follows:

$$H(p,u) = L(u) - L(u_0) + pL(u_0) + \frac{1}{\left((1+\alpha^{-1}) + \frac{\beta}{2}\right)} p\left(-\frac{\partial P}{\partial x} - \left(\frac{1}{Da} + M^2\right)u + \beta \frac{\partial N}{\partial y} - \left(M + \frac{1}{Da}\right)u + G_t\theta - G_f\varphi\right), \quad (17)$$

$$H(p,N) = L(N) - L(N_0) + pL(N) - \frac{1}{\gamma} p\left(2\beta N + \beta \frac{\partial u}{\partial y}\right), \quad (18)$$

$$H(p,\theta) = L(\theta) - L(\theta_0) + pL(\theta_0) + \frac{3p}{(3+4R)}\left(\frac{E_c P_r}{R_e}\left((1+\alpha^{-1}) + \frac{\beta}{2}\right)\left(\frac{\partial u}{\partial y}\right)^2 + N_t P_r \left(\frac{\partial \theta}{\partial y}\right)^2 + N_b P_r \left(\frac{\partial \varphi}{\partial y}\frac{\partial \theta}{\partial y}\right) + \frac{2\,\beta\, E_c}{R_e}\left[N^2 + N\frac{\partial u}{\partial y}\right] + \gamma \frac{E_c P_r}{R_e}\left(\frac{\partial N}{\partial y}\right)^2\right), \quad (19)$$

$$H(p,\varphi) = L(\varphi) - L(\varphi_0) + pL(\varphi) + p\frac{N_t}{N_b}\left(\frac{\partial^2 \theta}{\partial y^2}\right), \quad (20)$$

With $L = \frac{\partial^2}{\partial y^2}$ as the linear operator. The initial guess u_0, θ_0, N_0 and φ_0 can be written as

$$u_0 = -1, \theta_0 = \frac{-1}{h+\gamma_1}\, y, \varphi_0 = N_0 = \frac{y}{h}, \quad (21)$$

Now, it is assumed that:

$$(u,\theta,N,\varphi) = (u_0,\theta_0,N_0,\varphi_0) + p(u_1,\theta_1,N_1,\varphi_1) + p^2(u_2,\theta_2,N_2,\varphi_2) + \ldots\ldots . \quad (22)$$

The solutions of axial velocity, temperature, the micro-rotation velocity and nanoparticle volume friction are:

$$u(y) = -1 + a_0 + a_1 y + a_2 y^2 + a_3 y^3 + a_4 y^4 + a_5 y^5 + a_6 y^6, \quad (23)$$

$$\theta(y) = a_7 + a_8 y + a_9 y^2 + a_{10} y^3 + a_{11} y^4 + a_{12} y^5 + a_{13} y^6, \quad (24)$$

$$N(y) = a_{14} + a_{15} y + a_{16} y^2 + a_{17} y^3 + a_{18} y^4 + a_{19} y^5, \quad (25)$$

$$\varphi(y) = a_{20} + a_{21} y + a_{22} y^2 + a_{23} y^4. \quad (26)$$

Now reduced Nusselt number Nu and Sherwood number Sh at the wavy wall of the channel, are defined as

$$\tau_{xy} = (1+\alpha^{-1})\frac{\partial u}{\partial y}, \qquad Nu = \left.\frac{\partial \theta}{\partial y}\right|_{y=h},$$

$$Sh = \left.\frac{\partial \varphi}{\partial y}\right|_{y=h}. \quad (27)$$

The expressions for τ_{xy}, Nu and Sh have been obtained by substituting from Eqs. (23), (24) and (26) into Eq. (27) respectively, and they have been evaluated numerically for several values of the parameters of the problem, using the software Mathematica package. The obtained results will be discussed in the next section.

5. Results and discussion

In this research, we introduced the results of this problem with long wavelength approximation and low Reynolds number, i.e. the parameter δ assumed to be very small. Moreover, the default values of problem relevant parameters are taken as $\frac{\partial p}{\partial x} = 10, \alpha = 0.7, \beta = 0.5, G_t = 3, , G_f = 2, M = 10, \mathrm{Da} = 0.1, \mathrm{r} = 1, \mathrm{Ec} = 3.5, \mathrm{Pr} = 1.5, re = 0.01, \mathrm{Nt} = 3.5, \mathrm{Nb} = 2.5, \Upsilon = 1.2, \beta_1 = 0.01; \beta_2 = 0.05 , \Upsilon_1 = 0.1, \mathrm{h} = 1.2$.

Figs. (1) and (2) give the effects of the first order slip parameter β_1 and magnetic parameter M on the axial velocity u. It seen from these figures that the velocity increases as β_1 increases while it decreases as M increases. It is also noted that for each value of both β_1 and M, the axial velocity has a maximum value, i.e. u decreases as y increases till a maximum value, which increases by increasing β_1 and decreases by increasing M, and all maximum values occur at $y = 0.2$. The following clarifies the result in figure (2); the velocity of the fluid decreases in the fluid domain with increasing values of magnetic parameter due to the Lorentz force where the magnetic field opposes the transport phenomena where this force causes reduction in the fluid velocity within the boundary of tube wall. Moreover, the results are in a good agreement with those obtained by [34]. The effects of both β_2 and α on the velocity are found to be similar to effect of β_1 on the velocity u given in the figure (1) with the only difference that the obtained curves are very closer than those obtained in figure (1). But, these figures are excluded here to save space.

The influences of both the dimensionless viscosity ratio β and pressure gradient $\frac{\partial p}{\partial x}$ on the micro-rotation velocity N are represented in Figs. (3) and (4). It is shown from these figures that the micro-rotation velocity N increases as β increases while it decreases by the increasing of $\frac{\partial p}{\partial x}$. Moreover, for small values of β and large values of $\frac{\partial p}{\partial x}$., the relation between the micro-rotation velocity N and the transverse coordinate y is a semi-linear relation. The ratio ($\beta = k_1/\mu_f$) controls the relative might of the whirlpool viscosity coefficient to the coefficient of dynamical viscosity. These coefficients μ_f and k_1 should be greater or equal to zero. For example, μ_f =0.0029 and k_1=0.000232 in blood [30]. The vortex viscosity recedes energy very slowly but surely from the vortex core. It is only through dispersion of a vortex due to viscosity that a line of vortex can have a limit in the fluid. When the viscous effects are much larger than the spin gradient viscosity effects, (k_1/μ_f) may be tends to zero. All the above illustrate the result in figure (4).

The variation of temperature θ with the transverse coordinate y for different values of thermophoresis parameter Nt and Brownian motion parameter Nb are given in Figs. (5) and (6), respectively. These figures show that the temperature θ decreases by increasing Nt, whereas it increases by increasing Nb, in the interval y∈ [0, 0.7], otherwise, namely, after y = 0.7, it has an opposite behavior, i.e. the behavior of θ in the interval y∈ [0, 0.7], is an inversed manner of its behavior in the interval y∈ [0.7, 1.2] except that the curves are quietly close to each other in the second interval than those obtained in the first interval. In this case, for small values of Nb and large values of Nt, there is a maximum value of θ holds at y =0.95. The following interprets the result in figure (6); the more energetic the molecule's Brownian motion, the higher the temperature we sense. Absolute temperature is proportional to Brownian motion' kinetic energy per unit mass in a more specific way. So, if we raise the temperature, Brownian motion becomes more energetic. The effects of thermal Grashoff number Gt and slip temperature parameter Υ_1 on the temperature distribution θ are shown in Figs. (7) and (8), respectively. It is clear from these figures that the effect of Gt and Υ_1 on the temperature is similar to the effect of Nb and Nt on θ in the first interval, respectively. It is also noted that for large values of Gt and small values of Υ_1, the temperature distribution has a maximum value, i.e. θ increases as y increases till a maximum value. After this maximum value, the temperature θ will decrease, and all maximum values occur at y= 0.9. The effects of both Gf and Υ on the temperature are found to be similar to effect of Gt on the temperature θ given in the figure (7); these figures are excluded here to avoid any kind of repetition.

Figures (9) and (10) illustrate the change of the nanoparticle concentration φ versus the transverse coordinate y with several values of the radiation parameter R and Eckert number Ec, respectively. It is seen from these figures that the nanoparticle concentration increases with the increasing of R, whereas it decreases as Ec increases. It is also noted that the nanoparticle concentration for different values of R and Ec becomes lower as y increases and reaches a minimum value (at a finite value of y: $y = y_0$) after which it increases, and all minimum values occur at y=0.6. It is also observed from Fig. (10) that there is a drop in the nanoparticle concentration due to the heat generated by the viscous dispersion and it is in agreement with the fact that the power is stored in a definite area of fluid due to portional heating as a consequence of dispersion due to viscosity, and hence the nanoparticle concentration decreases as Ec increases. The effects of γ and Pr on the nanoparticle concentration are found to be similar to the effect of Ec given in Fig. (10), and there are only two differences, the first one is that the obtained curves are

very close to those obtained in Fig. (10). Morevere, the effect of Gt and Br on nanoparticle concentration is bounded.

The effects of Eckert number Ec and the second slip parameter β_2 on the entropy generation which is a function of the transverse coordinate y are shown in Figs. (11) and (12). It is shown that the entropy generation Eg increases as Ec increases whereas it decreases as β_2 increases. Moreover, the obtained curves don't intersect at the boundary of channel; this is due to the boundary conditions given in (15), and they are coincide near the axis of channel, namely in the interval y∈ [0, 0.35].

Fig(1)

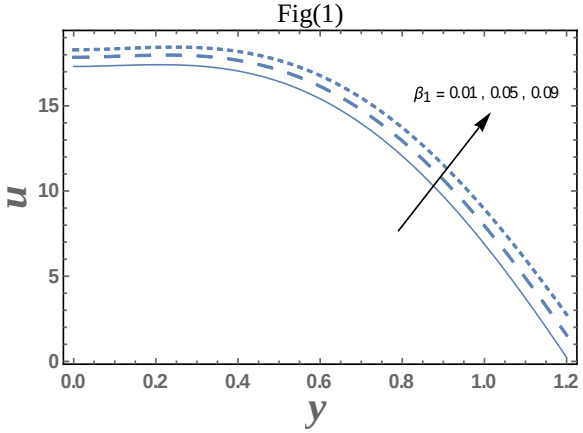

Fig(2)

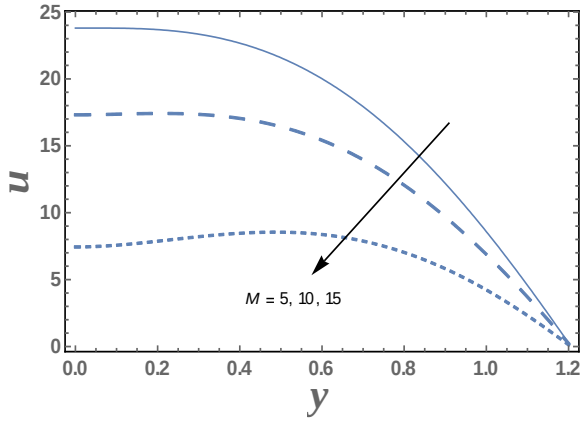

Fig(3)

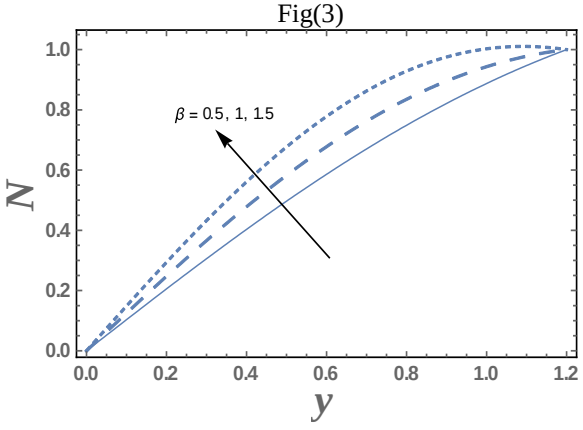

Fig(4)

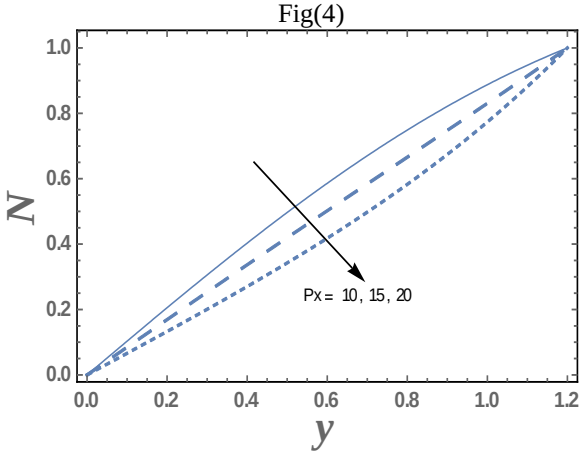

Fig(5)

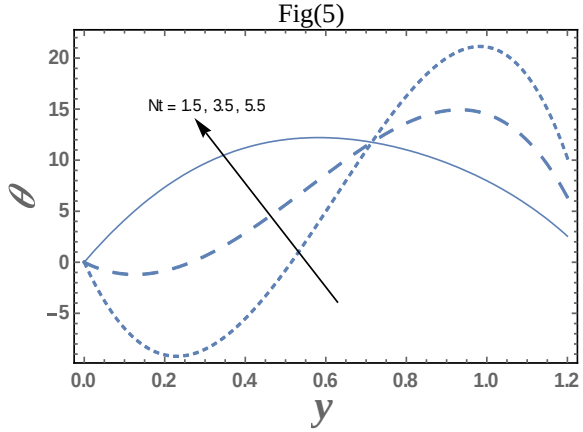

Fig(6)

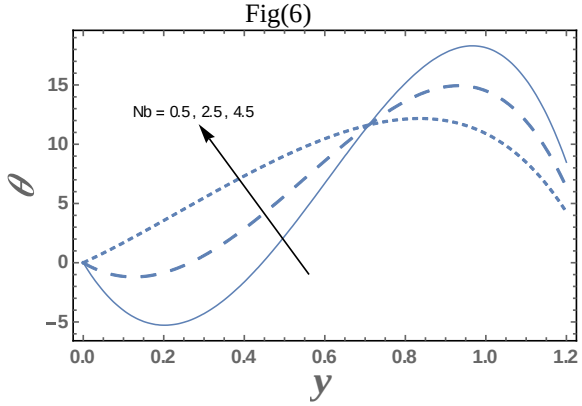

Fig(7)

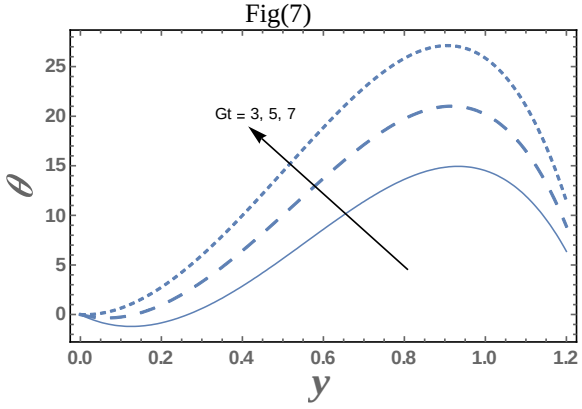

Fig(8)

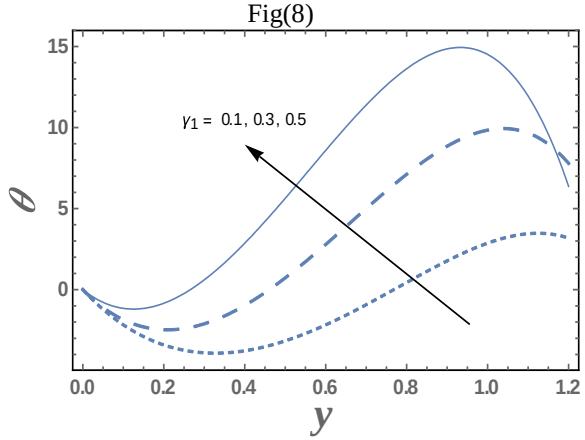

Fig(9)

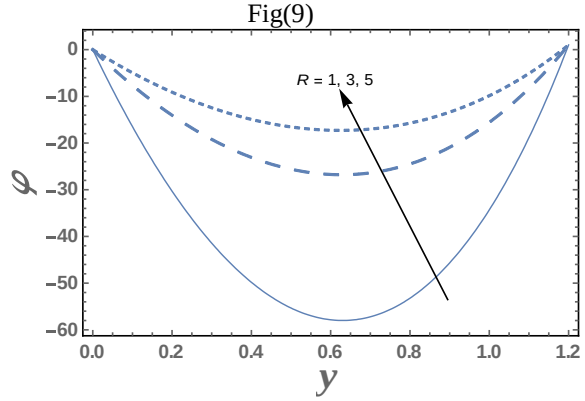

Fig(10)

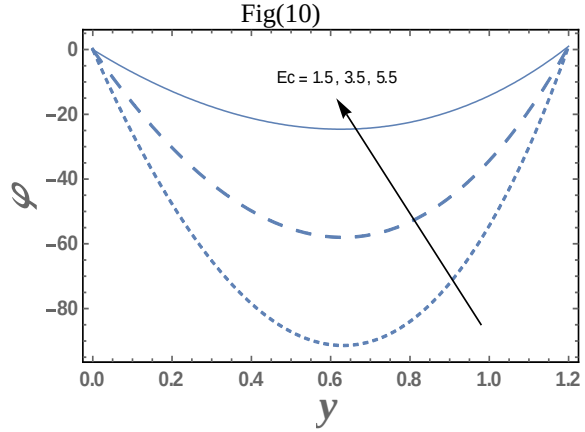

Fig(11)

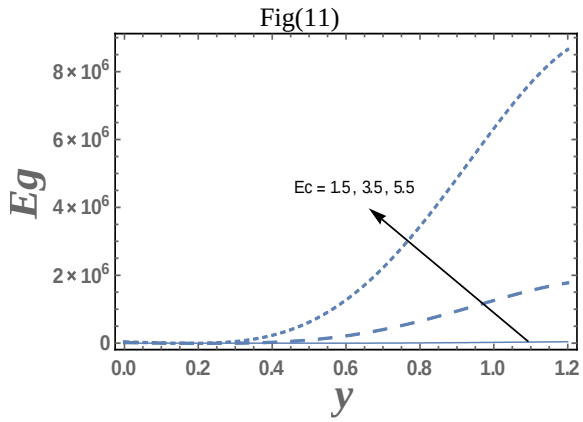

Fig(12)

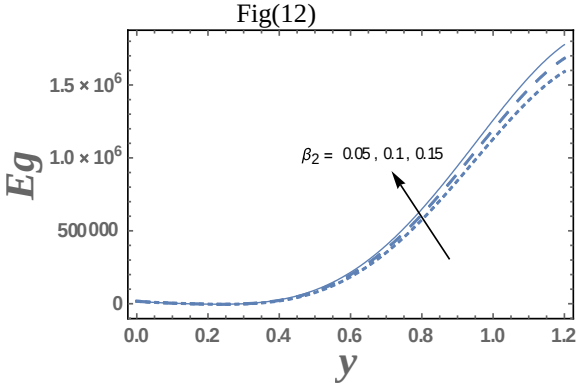

5. Conclusion

The main aim of this paper is to study MHD peristaltic flow of micropolar biviscosity nanofluid through a porous media with entropy generation effect. In our analysis, the effects of radiation, viscous dissipation and mixed convection are taken into account. The analytical expressions are constructed for the axial velocity, microrotation velocity, temperature and nanoparticles concentration distributions. Also, the skin friction, Nussselt number and Sherwood number at the wavy wall of the channel are obtained. Many physiological flows can be presented by this model [35-38]. The major findings can be briefed as follows:

(1) The axial velocity u increases as Ec, β, Nt, and γ increase, but it decreases with the increasing of R, Re and Nb .

(2) The axial velocity u becomes lower with increasing the coordinate y and reaches minimum value (at a finite value of y : $y = y_0$) after which it increases

(3) As β and α increase, the microrotation velocity N increases, while it decreases with the increase of Da, Gt, and Gf.

(4) The temperature θ increases with the increase each of Da, Gf, Gt and γ, whereas it decreases as M, β , α and γ_1 increase.

(5) The temperature θ becomes greater with increasing the coordinate y and reaches maximum value (at a finite value of y : $y = y_0$) after that it decreases.

(6) The nanoparticles concentration φ has an opposite behavior compared to temperature behavior except that it has the same behavior at the channel boundary.

(7) By increasing each of Da, Pr, Ec, β, γ_1, Gt and G_f, the entropy generation Eg increases, while it decreases as α, β_1, β_2, M and R increase. Furthermore, the obtained curves don't intersect at the channel boundary, this occurs due to the boundary conditions of the problem.

.

References

[1] M. El. Ouaf and M. Abou-zeid, Electromagnetic and non-Darcian effects on a micropolar non-Newtonian fluid boundary-layer flow with heat and mass transfer, *International Journal of Applied Electromagnetics and Mechanics* **66** (2021), 693-703.

[2] K. Aslani and I. Sarris, Effect of micromagneto-rotation on the heat transfer of micropolar Hartmann flow, *Thermal Science and Engineering Progress* **26** (2021), 101129.

[3] N. T. Eldabe, M. Y. Abou-zeid, O. H. El-Kalaawy, S. M. Moawad and O.S Ahmed, Electromagnetic steady motion of Casson fluid with heat and mass transfer through porous medium past a shrinking surface, *Thermal Science* **25**(1A) (2021), 257-265.

[4] B. Ali, A. Shafiq, I. Siddique, Q. Al-Mdallal, F.Jarad, Significance of suction/injection, gravity modulation, thermal radiation, and magnetohydrodynamic on dynamics of micropolar fluid subject to an inclined sheet via finite element approach, *Case Studies in Thermal Engineering* **28** (2021) 101537.

[5] M. Y. Abou-zeid, Effects of thermal-diffusion and viscous dissipation on peristaltic flow of micropolar non-Newtonian nanofluid: Application of homotopy perturbation method, *Results in Physics* **6** (2016), 481-495.

[6] G. Sofiadis and I. Sarris, Microrotation viscosity effect on turbulent micropolar fluid channel flow, *Physics of Fluids* **33** (2021), 095126.

[7] J. Su, Suitable weak solutions to the micropolar fluids model in a bounded domain, *Journal of Mathematical Analysis and Applications* **504** (2021), 125406.

[8] N. T. Eldabe and M. Abou-zeid, Magnetohydrodynamic peristaltic flow with heat and mass transfer of micropolar biviscosity fluid through a porous medium between two co-axial tubes, *Arabian Journal for Science and Engineering* **39** (2014), 5045-5062.

[9] O. Chun, M. A. Z. Raja, S. Naz, I. Ahmad, R. Akhtar, Y. Ali, and M. Shoaib, , Dynamics of inclined magnetic field effects on micropolar Casson fluid with Lobatto IIIA numerical solver, *AIP Advances* **10** (2020), 065023.

[10] N. T. M. Eldabe, M. Y. Abou-zeid, S. M. Elshabouri, T. N. Salama and A. M. Ismael, Ohmic and viscous dissipation effects on micropolar non-Newtonian nanofluid Al2O3 flow through a non-Darcy porous media, Int. J. Appl. Electromag. Mech. **68** (2022), 209-221.

[11] N. T. M. Eldabe, R. R. Rizkallah, M. Y. Abou-zeid and V. M. Ayad, Thermal diffusion and diffusion thermo effects of Eyring- Powell nanofluid flow with gyrotactic microorganisms through the boundary layer, *Heat Transfer - Asian Res*. **49** (2020), 383 – 405.

[12] O. Mahian, E. Bellos, C. N. Markides, R. A. Taylor, A. Alagumalai, L. Yang, G. Ahmadi, S. Wongwises, C.Qin and B. J. Lee, Recent Advances in Using Nanofluids in Renewable Energy Systems and the Environmental Implications of their Uptake**,** *Nano Energy* **86**(4) (2021), 106069.

[13] M. El. M. Ouaf and M. Y. Abou-zeid, Hall currents effect on squeezing flow of non-Newtonian nanofluid through a porous medium between two parallel plates, *Case Studies in Thermal Engineering* **28**(2021), 101362.

[14] N. T. M. Eldabe, M. Y. Abou-zeid, M. A. A. Mohamed and M. M. Abd-Elmoneim, MHD peristaltic flow of non-Newtonian power-law nanofluid through a non-Darcy porous medium inside a non-uniform inclined channel, *Archive of Applied Mechanics* **91** (2021), 1067–1077.

[15] J. P. Vallejo, J. I. Prado and L. Lugo, Hybrid or mono nanofluids for convective heat transfer applications. A critical review of experimental research, *Applied Thermal Engineering* **203** (2022), 117926.

[16] M. Y. Abou-zeid, Implicit homotopy perturbation method for MHD non-Newtonian nanofluid flow with Cattaneo-Christov heat flux due to parallel rotating disks, *Journal of nanofluids* **8**(8) (2019), 1648-1653.

[17] N. T. Eldabe, G. M. Moatimid, M. Y. Abouzeid, A. A. ElShekhipy and N. F. Abdallah, A semianalytical technique for MHD peristalsis of pseudoplastic nanofluid with temperature-dependent viscosity: Application in drug delivery system, *Heat Transfer-Asian Research* **49 (**2020), 424– 440.

[18] N. T. M. Eldabe, G. M. Moatimid, M. Abou-zeid, A. A. Elshekhipy and N. F. Abdallah, Semi-analytical treatment of Hall current effect on peristaltic flow of Jeffery nanofluid, Int. J. Appl. Electromag. Mech. **7** (2021), 47-66.

[19] N. T. M. Eldabe, M. Y. Abou-zeid, A. Abosaliem, A. Alana, and N. Hegazy, Homotopy perturbation approach for Ohmic dissipation and mixed convection effects on non-Newtonian nanofluid flow between two co-axial tubes with peristalsis, Int. J. Appl. Electromag. Mech. **67** (2021), 153-163.

[20] N. T. Eldabe, M. Y. Abou-zeid, M. A. Mohamed and M. Maged, Peristaltic flow of Herschel Bulkley nanofluid through a non-Darcy porous medium with heat transfer under slip condition,

Int. J. Appl. Electromag. Mech. **66** (2021), 649-668.

[21] N. T. M. Eldabe, G. M. Moatimid, M. Abou-zeid, A. A. Elshekhipy and N. F. Abdallah, Instantaneous thermal-diffusion and diffusion-thermo effects on Carreau nanofluid flow over a stretching porous sheet, *Journal of Advanced Research in Fluid Mechanics and Thermal Sciences* **72** (2020) 142-157.

[22] P.S. Salimath, I.S. Ertesvag, Local entropy generation and entropy fluxes of a transient flame during head-on quenching towards solid and hydrogen-permeable porous walls, *International Journal of Hydrogen Energy* **46** (52) (2021), 26616-26630.

[23] U. Farooq, H. Waqas, M. Imran, M. Alghamdi and T. Muhammad, On melting heat transport and nanofluid in a nozzle of liquid rocket engine with entropy generation, *Journal of material sresearch and technology* **14** (2021), 3059-3069.

[24] X.Chen, Y. Jian, Entropy generation minimization analysis of two immiscible fluids, *International Journal of Thermal Sciences* **171** (2022), 107210-107219.

[25] S.K. Asha, C.K. Deepa, Entropy generation for peristaltic blood flow of a magneto- micropolar fluid with thermal radiation in a tapered asymmetric channel, *Results in Engineering* **3** (2019), 100024.

[26] B. Darbari, S. Rashidi and A. Keshmiri, Nanofluid heat transfer and entropy inside a triangular duct equipped with delta winglet vortex generators, *Journal of Thermal Analysis and Calorimetry* **140** (2020), 1045–1055.

[27] T. Hayat, S.Nawaz, A. Alsaedi and O. Mahian, Entropy generation in peristaltic flow of Williamson nanofluid, *Physica Scripta* **94** (2019), 125216.

[28] G. Mandal and D. Pal, Entropy Generation Analysis of Radiated Magnetohydrodynamic Flow of Carbon Nanotubes Nanofluids with Variable Conductivity and Diffusivity Subjected to Chemical Reaction, *Journal of Nanofluids* **10** (2021) 491–505.

[29] A.O. Adelaja, J. Dirker and J.P. Meyer, Experimental study of entropy generation during condensation in inclined enhanced tubes, *International Journal of Multiphase Flow* **145** (2021), 103841.

[30] N. T. M. Eldabe, M. Y. Abou-zeid, M. E. Ouaf, D. R. Mustafa and Y. M. Mohammed, Cattaneo – Christov heat flux effect on MHD peristaltic transport of Bingham Al_2O_3 nanofluid through a non – Darcy porous medium Int. J. Appl. Electromag. Mech. **68** (2022), 59-84.

[31] Eldabe NT, Shaaban AA, Abou-Zeid MY, Ali HA. MagnetohydrodynamicNon-Newtonian Nanofluid Flow Over a Stretching Sheet Through a Non-Darcy Porous Medium with Radiation and Chemical Reaction. Journal of Computational and Theoretical Nanoscience **12** (2015), 12:5363-5371.

[32] M.Y. Abou-zeid, Homotopy perturbation method to gliding motion of bacteria on a layer of power-law nanoslime with heat transfer, Journal of Computational and Journal of Computational and Theoretical Nanoscience **12** (2015), 12:3605-3614.

[33] M. A. Mohamed and M.Y. Abou-zeid, MHD peristaltic flow of micropolar Casson nanofluid through a porous medium between two co-axial tubes, *J. porous media* **22** (2019), 1079–1093.

[34] N T. Eldabe and M. Y. Abou-Zeid, Radially varying magnetic field effect on peristaltic motion with heat and mass transfer of a non-Newtonian fluid between two co-axial tubes, Thermal Science **22** (6A) (2018), 2449-2458.

[35] M. A. Batiha, M. M. Dardir, H. Abuseda, N. A. Negm and H. E. Ahmed, Improving the performance of water-based drilling fluid using amino acid-modified graphene oxide nanocomposite as a promising additive, Egyptian Journal of Chemistry **64** (2021), 1799-1806.

[36] Hany E. Ahmed, Mohamed A. Betiha, Mona El-Dardir, Modather F. Hussein and Nabel Negm, High-Performance Rheology Modifiers and Fluid Loss of Starch-Bentonite Mixed System in Mud Fluids: Experimental and Optimization Study, Egyptian Journal of Chemistry **64** (2021), 1653-1664.

[37] W. Abbas, Nabil T. M. Eldabe, Rasha A. Abdelkhalek, Nehad, A. Zidan and S. Y. Marzouk, Soret and Dufour Effects with Hall Currents on Peristaltic Flow of Casson Fluid with Heat and Mass Transfer Through Non-Darcy Porous Medium Inside Vertical Channel, Egyptian Journal of Chemistry **64** (2021), 5217-5227.

[38] Rajaa Mohammad, Sabeeh Jassim and Luma Ahmed, Halogens Substitution Effects on Electronic and Spectral Properties of Carbon Nanotube Molecules studying with the DFT method, Egyptian Journal of Chemistry **64** (2021), 3587-3595.